Shear Flows in Far-from-Equilibrium Strongly Coupled Fluids

Matteo Baggioli,[1,2,*] Li Li,[3,4,5,†] and Hao-Tian Sun[3,4,‡]

[1]Wilczek Quantum Center, School of Physics and Astronomy, Shanghai Jiao Tong University, Shanghai 200240, China
[2]Shanghai Research Center for Quantum Sciences, Shanghai 201315, China
[3]CAS Key Laboratory of Theoretical Physics, Institute of Theoretical Physics, Chinese Academy of Sciences, Beijing 100190, China
[4]School of Physical Sciences, University of Chinese Academy of Sciences, Beijing 100049, China
[5]School of Fundamental Physics and Mathematical Sciences, Hangzhou Institute for Advanced Study, University of Chinese Academy of Sciences, Hangzhou 310024, China

(Received 24 December 2021; revised 14 April 2022; accepted 10 June 2022; published 27 June 2022)

Although the viscosity of a fluid ranges over several orders of magnitude and is extremely sensitive to microscopic structure and molecular interactions, it has been conjectured that its (opportunely normalized) minimum displays a universal value which is experimentally approached in strongly coupled fluids such as the quark-gluon plasma. At the same time, recent findings suggest that hydrodynamics could serve as a universal attractor even when the deformation gradients are large and that dissipative transport coefficients, such as viscosity, could still display a universal behavior far from equilibrium. Motivated by these observations, we consider the real-time dissipative dynamics of several holographic models under large shear deformations. In all the cases considered, we observe that at late time both the viscosity-entropy density ratio and the dimensionless ratio between energy density and entropy density approach a constant value. Whenever the shear rate in units of the energy density is small at late time, these values coincide with the expectations from near equilibrium hydrodynamics. Surprisingly, even when this is not the case, and the system at late time is far from equilibrium, the viscosity-to-entropy ratio approaches a constant which decreases monotonically with the dimensionless shear rate and can be parametrically smaller than the hydrodynamic result.

DOI: 10.1103/PhysRevLett.129.011602

Introduction.—Viscosity measures the resistance of a fluid to shearing motion and represents one of the most fundamental properties of liquid dynamics, whose importance ranges from biology and chemistry to cosmology and relativistic heavy-ion collisions. Although its value spans many orders of magnitude and strongly depends on the microscopic interactions and structure, its minimum displays a certain degree of universality. This was first suggested by Purcell [1,2] and then emphasized in the famous Kovtun-Son-Starinets (KSS) bound [3] which has already found numerous experimental confirmations [4–7] (see Ref. [8] for a review). The universal character has also been generalized to different diffusive processes [9] and recently confirmed in a large class of nonrelativistic liquids [10–12].

From a dynamical perspective, the viscosity η specifies the relation between the shear stress σ and the rate of shear deformation $\dot{\gamma}$:

$$\eta \equiv \frac{\sigma}{\dot{\gamma}}, \tag{1}$$

and, for small shear rates, it can be consistently assumed to be a constant. On the contrary, when the deformation rate becomes large, this remains true only for a small subclass of systems known as *Newtonian fluids*. In all other cases [13,14], the viscosity becomes a nonlinear function of the shear rate itself, producing a plethora of interesting and ubiquitous phenomena such as *shear thickening*, *shear thinning*, and many more. Familiar examples of non-Newtonian fluids are whipped cream, wall paints, blood, and wet sand. In these scenarios, it is customary to define an apparent viscosity $\sigma = \eta(\dot{\gamma})\dot{\gamma}$ which converges to the near-equilibrium viscosity η_0 only in the limit $\dot{\gamma}\tau \ll 1$ (where τ is the characteristic relaxation time of the system), and that can be easily measured in rheological experiments using a viscometer.

Importantly, whenever the shear rate is large with respect to the characteristic energy scale of the system, the fluid finds itself in a far-from-equilibrium state that cannot be described by linearized hydrodynamics, intended as the effective description of the long wavelength and late-time physics, and which *a priori* is not expected to reveal any degrees of universality. Interestingly, the early-time

dynamics of the quark-gluon plasma (QGP), the most perfect fluid in nature [15,16] is characterized by large spatial gradients [17]. Its far-from-equilibrium nature [18] renders the applicability of hydrodynamics questionable (see Refs. [19,20] for reviews about the topic).

In recent years, there has been an incredible effort in understanding whether hydrodynamics, and in which form exactly, can be still useful and applicable to describe the far-from-equilibrium dynamics of fluids [21–23], leading to new ideas at the edge between math and physics, such as resummed transport coefficients [24], hydrodynamics attractors [25–27], resurgent transseries [28], and many more. Holography [29–31] represents a very natural playground to test and explore these ideas by performing controllable computations of the real-time far-from-equilibrium dynamics of strongly coupled fluids [21,32–43].

The current interpretation suggests that hydrodynamics may still be defined as a *universal attractor* [44–48] and that dissipative transport coefficients, such as viscosity, can still show a universal behavior even when local gradients are large and the system is far from equilibrium. Following this paradigm, a natural question to ask is whether there is any remnant of the universal KSS bound far from equilibrium, i.e., for large shear rates. In particular, one would like to understand whether the dimensionless viscosity-entropy density ratio, when opportunely defined, remains constant far from equilibrium and whether such a value coincides or not with the KSS bound $\eta_0/s = 1/4\pi$ (with $\hbar = k_B = 1$). Here, η_0 is the value of the viscosity defined within linear response in the hydrodynamic limit and appearing as a first-order dissipative correction to the stress-energy tensor T^{ab} [49]. Importantly η_0 is different from η in Eq. (1) for large shear rates.

In this Letter, we consider the real-time dynamics of several bottom-up holographic models under large shear deformations, which correspond to large N strongly coupled fluids far from equilibrium. By considering time-dependent backgrounds with finite shear deformations, we analyze the behavior of the viscosity under large gradients and explore to which extent its universal character is preserved when the system is driven far away from the equilibrium state.

Shear flows, viscosity, and thermodynamics.—Near equilibrium, where linearized hydrodynamics applies, the viscosity can be extracted in terms of the stress tensor retarded Green's function using the standard Kubo formula [50]:

$$\eta_0 = -\lim_{\omega\to 0}\frac{1}{\omega}\mathrm{Im}[\mathcal{G}^{(\mathrm{R})}_{T_{xy}T_{xy}}(\omega)], \tag{2}$$

where, for simplicity, only two spatial dimensions (x, y) are considered. This procedure can be easily implemented in the holographic formalism by considering an infinitesimal gravitational shear perturbation $\delta g_{xy} \sim e^{-i\omega t}$ and computing the linear retarded response of the dual stress tensor using the holographic dictionary [51–53]. In general, whenever the shear strain rate $\dot{\gamma}$ is large, both the linear response formalism and the hydrodynamics approximation are not applicable anymore, and thus the Kubo formula in Eq. (2) loses its meaning. In this situation, in which the gravitational solution becomes inherently time dependent, a more appropriate and robust way of proceeding is to compute directly the time-dependent boundary stress tensor σ which is now a nonlinear function of $\dot{\gamma}$, and apply the more general formula presented in Eq. (1). As a result, the apparent viscosity η is generally a function of both time and shear rate, thus displaying a much richer dynamics than its near equilibrium counterpart η_0. This is the procedure that will be adopted in this work.

In time-dependent holographic solutions, or equivalently in field theories out of equilibrium, aside from the definition of the viscosity, one must be extremely careful with the definitions of the thermodynamic quantities such as the temperature and entropy [54–56]. The standard definition of entropy, extracted using the Bekenstein-Hawking law from the area of the black-hole event horizon [57], becomes questionable. Nevertheless, there is increasing evidence (see Ref. [58] for a detailed discussion on this point) that the correct derivation of the entropy density in out-of-equilibrium gravitational systems is through the area of the apparent horizon that is defined using local quantities [59]. We will therefore follow this identification. Importantly, because of the large N limit, the effects of hydrodynamic fluctuations which are known to spoil the late-time behavior of two dimensional fluids [60] are neglected in our computations. We do expect the picture emerging from our analysis to be, at least qualitatively, similar to that in higher dimensions where the effects of fluctuations become irrelevant.

Out-of-equilibrium steady states.—We consider three different bottom-up models in asymptotically AdS_4 spacetime. The first setup is the standard Einstein-Maxwell (EM) action whose field theory dual represents a $(2+1)$ dimensional strongly coupled relativistic charged fluid with a global U(1) symmetry [61]. The second framework contains a different deformation which introduces a nontrivial elastic bulk modulus in the neutral dual field theory (see Refs. [62–67] for more details). Finally, in the third one, conformal symmetry is explicitly broken by a scalar deformation, and the corresponding boundary stress tensor is no longer traceless [68]. Near equilibrium (in the hydrodynamic limit), all the dual fluid field theories considered display a universal value for the viscosity-to-entropy density ratio which saturates the KSS bound $\eta_0/s = 1/4\pi$. All the additional details about the models can be found in the Supplemental Material [69].

In order to drive our holographic systems far from equilibrium, we introduce a time-dependent source for the metric component g_{xy}. From the dual field theory point

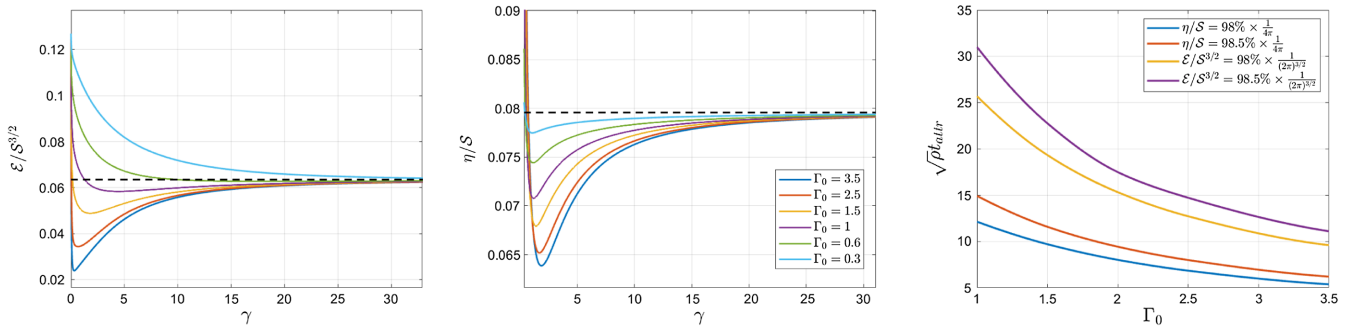

FIG. 1. Left: $\mathcal{E}/\mathcal{S}^{3/2}$ as a function of $\gamma(t)$, where the dash line is $1/(2\pi)^{3/2}$. Center: $\eta/\mathcal{S}$ as a function of $\gamma(t)$, where the dash line is $1/4\pi$. Right: The dimensionless attracting times, defined using the 1.5% and 2% rules, for both the viscosity and energy density ratios as a function of the normalized shear rate.

of view, that corresponds to deforming our fluid with a time-dependent shear strain $\gamma(t)$. In the main text, we will focus on the EM model and two benchmark shear rates. Different holographic models (including a nonconformal one) and different shear strain deformations are discussed in the Supplemental Material [69] and give equivalent results. We construct numerically the far-from-equilibrium geometry which allows us to read all the physical observables of the dual field theory. Importantly, because the boundary field theory geometry is not of Minkowski type, extra care needs to be taken in order to define the boundary shear stress $\sigma(t)$ and the shear strain $\gamma(t)$. All the details of our computations can be found in the Supplemental Material [69].

Let us first consider the EM model in the presence of a constant shear rate $\dot{\gamma} \equiv \gamma_0$. The time-dependent dynamics (see Fig. SI1 in the Supplemental Material [69]) strongly depends on the dimensionless shear rate $\Gamma_0 \equiv \gamma_0/\sqrt{\rho}$, where ρ is the charge density of the dual field theory. For small Γ_0, the time evolution is slow, and all quantities slowly grow in time. Whenever the gradients are large, all quantities rapidly increase and deviate from their initial values. The viscosity and the entropy density grow quadratically in time $\sim t^2$ while the energy density grows like $\sim t^3$. More in general, we find that, independently of the shear deformation used, the behavior of the energy density is constrained by one of the Einstein's equations as follows:

$$\mathcal{E}(t) - \mathcal{E}_{\rm ini} = \int_{t_{\rm ini}}^{t} \dot{\gamma}(\tau)\sigma(\tau)d\tau = \int_{t_{\rm ini}}^{t} \eta(\tau)\dot{\gamma}(\tau)^2 d\tau, \qquad (3)$$

from which the cubic scaling mentioned above can be immediately derived. Here, the subscript *ini* refers to the initial configuration on top of which the shear deformation is switched on. Equation (3), which is obtained analytically from the gravitational setup (see the Supplemental Material [69]), corresponds exactly to the expression for the dissipated energy in a viscoelastic system under deformations [70]. Let us emphasize that, in order to avoid infinite gradients during the introduction of the constant strain rate, the time-dependent boundary strain $\gamma(t)$ presents an initial activation window which is responsible for the nonmonotonic oscillations observed in all our results at early time. We explicitly checked that the form of the activation function does not affect our results.

From a physical perspective, we can notice that the apparent viscosity η grows with the shear rate Γ_0. In the context of rheology, this behavior is denoted as *shear thickening*, and it is typical of dilatant fluids, such as blood, ketchup, and peanut butter. These results are compatible with those of Ref. [71], found using oscillatory strain methods.

The dynamics of the two dimensionless ratios $\mathcal{E}/\mathcal{S}^{3/2}$, $\eta/\mathcal{S}$, with $\mathcal{S}$ the entropy density, is shown in Fig. 1. The time evolution profiles present a transient regime which is highly sensitive to the initial conditions and to the rate of shear deformation Γ_0. In that window, none of the quantities seem to follow any specific trend, and the UV microscopic details are dominating the dynamics. The deviations from the initial value can reach up to 50% and are larger by increasing the rate of deformation Γ_0. Moreover, the viscosity-to-entropy density ratio clearly violates the KSS bound in agreement with the results of Ref. [72]. Nevertheless, after a certain time, which we label as the *attracting time* (see below for a more formal definition), we observe that both quantities approach a constant value which is given exactly by the close-to-equilibrium hydrodynamics expectations. The same universal behavior is observed in the other holographic models considered and, surprisingly, also for a nonconformal model (see the Supplemental Material [69]) and for deformations with a nonconstant shear rate such as $\gamma(t) \sim \sqrt{t}, t^2, t^4$ (see Supplemental Material [69]).

To continue, let us define the *attracting time* $t_{\rm attr}$ as the value at which the dimensionless quantities reach their final late-time values. Pragmatically, we decided to use two different criteria coinciding with 98% and the 98.5% of the final values. We show this quantity for both the viscosity and the entropy density as a function of the normalized shear rate in the right panel of Fig. 1. Interestingly, we find

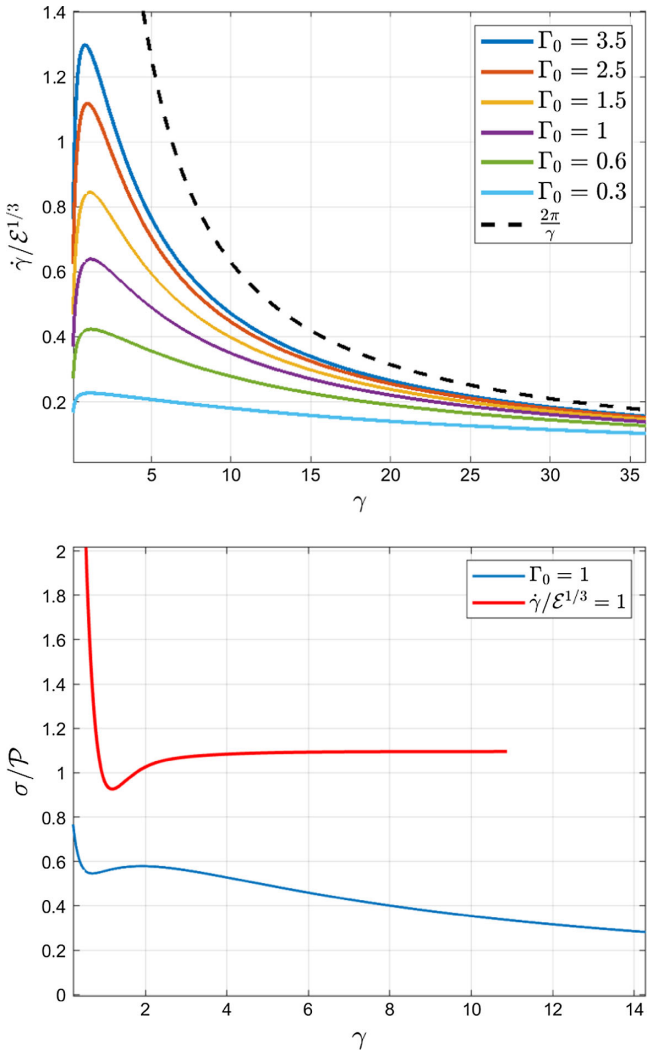

FIG. 2. Top: The dimensionless combination $\dot{\gamma}/\mathcal{E}^{1/3}$ as a function of γ for different shear rates. The dashed line is the attractor function $2\pi/\gamma$ approached by all curves for $\gamma \gg 1$. Bottom: The pressure anisotropy $\sigma/\mathcal{P}$ as a function of $\gamma(t)$ for constant $\Gamma_0 = 1$ (blue) and at constant $\dot{\gamma}/\mathcal{E}^{1/3} = 1$ (red) in the EM model.

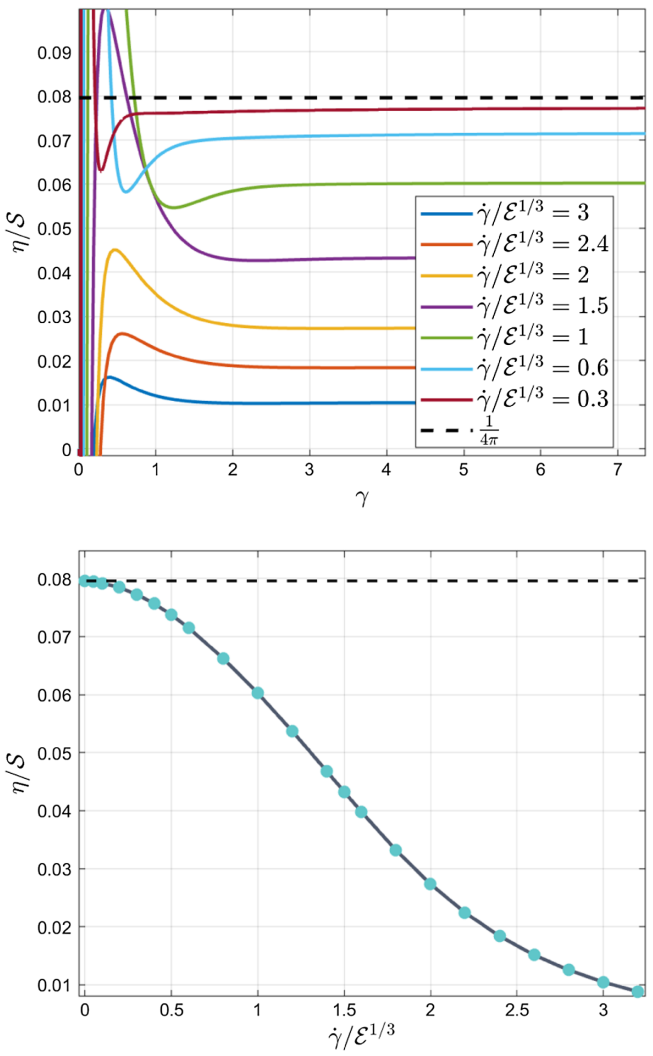

FIG. 3. The out-of-equilibrium steady state. Top: η/s as a function of γ for different values of the dimensionless gradient $\dot{\gamma}/\mathcal{E}^{1/3}$. Bottom: The value of the η/s ratio at late time as a function of the dimensionless shear rate $\dot{\gamma}/\mathcal{E}^{1/3}$.

that the larger the shear rate, the faster the time evolution reaches the universal attractor.

In order to understand this emerging universality, in Fig. 2, we plot the dimensionless ratio between the shear rate and the energy density of the system. We find that for large deformations $\gamma \gg 1$, such a ratio goes to zero following a universal law $\dot{\gamma}/\mathcal{E}^{1/3} = 2\pi/\gamma$. This numerical observation implies the existence of a universal attractor solution in the regime $\gamma(t) = \gamma_0 t \gg 1$ given by

$$\mathcal{E} = \left(\frac{\gamma_0}{2\pi}\right)^3 \gamma^3, \qquad \eta = \frac{\gamma_0^2}{2(2\pi)^2}\gamma^2, \qquad \mathcal{S} = \frac{\gamma_0^2}{2\pi}\gamma^2, \tag{4}$$

which is consistent with the data presented in Fig. 1.

Note that, in far-from-equilibrium systems, a local rest frame might be absent [73]. In all the cases considered, a local rest frame exists (see the Supplemental Material [69]) and therefore the notion of hydrodynamic attractor is always well defined [73].

A far-from-equilibrium case.—In the setups considered so far, the shear rate in units of the characteristic energy scale of the system becomes small at late time (see top panel of Fig. 2). This suggests the presence of a late-time steady state which is effectively in equilibrium. Therefore, it is perhaps not surprising that the near equilibrium hydrodynamic results apply in these situations.

By considering a different time-dependent shear rate (see details in the Supplemental Material [69]), we are able to keep the energy-normalized shear rate fixed, and arbitrarily large, at late time. In this case, the system never reaches an effective equilibrium state in which all physical quantities

are time dependent but the gradients are small compared with the characteristic energy scale. This distinction is confirmed by the analysis of the pressure anisotropy $\Delta\mathcal{P} \equiv \sigma/\mathcal{P}$ at late time, $\gamma \to \infty$ (bottom panel of Fig. 2). Whether for the previous cases (blue curve) $\Delta\mathcal{P} \to 0$ at late times, in this new setup (red curve) it approaches an $\mathcal{O}(1)$ constant signaling the far-from-equilibrium nature of the late-time state. Interestingly, even in this far-from-equilibrium situation, both the viscosity-to-entropy ratio and the dimensionless energy density approach a constant value in the late-time steady state, as shown in the top panel of Fig. 3. Nevertheless, this value does not coincide anymore with the near-equilibrium expectation, e.g., $1/4\pi$ for the viscosity. On the contrary, as shown in the bottom panel of Fig. 3, the out-of-equilibrium value for $\eta/\mathcal{S}$ decays monotonically with the strength of the shear gradient and seems to approach zero for extremely large values of the shear rate. This indicates that, even far from equilibrium, the system is described by an effective hydrodynamic steady state whose transport properties are nevertheless parametrically different with respect to its near-equilibrium counterpart. Our results are consistent with the findings of Ref. [74] for the highly symmetric Bjorken flow in which the viscosity out of equilibrium was found to be parametrically smaller than the equilibrium value.

Outlook.—In summary, we have performed an extensive time-dependent numerical analysis of several bottom-up (conformal and not) holographic models driven away from equilibrium by different shear rates. Whenever the shear rate in units of the energy density becomes small at late time, our results reveal the emergence of a universal attracting behavior, encoded in the simple solution [Eq. (4)], on which both the dimensionless viscosity-entropy and energy-entropy ratios reach a constant value which coincides exactly with the prediction of hydrodynamics naively valid only near equilibrium. Importantly, we prove that this behavior also persists when conformal symmetry is abandoned (see, e.g., Refs. [74–76] for similar discussions).

In the second scenario, in which the shear rate is kept constant and large in units of the energy density, we still observe a late-time steady state on which the $\eta/\mathcal{S}$ ratio takes a constant value. Nevertheless, we find that such a value does not coincide anymore with the near-equilibrium hydrodynamic result $1/4\pi$, but it rather decreases monotonically with the strength of the gradients, becoming parametrically smaller than the KSS bound.

Our results provide another case in favor of "the unreasonable effectiveness" [77,78] of a nonlinearly renormalized version of hydrodynamics out of equilibrium and might have important consequences not only on the out-of-equilibrium dynamics in heavy-ion collisions and QGP [20,23,79,80] but also on the understanding and characterization of the rheological response of complex fluids [65,71,81] using the holographic tool [82]. As a road map for the future, it would be interesting to understand whether the existence of the observed far-from-equilibrium steady states is universal and whether the corresponding transport properties can be related (probably in a highly nonlocal way) to the near equilibrium counterparts (e.g., by promoting the transport coefficients to be nonlinear functions of the deformations or by resumming the nonlinear effects).

We thank A. Buchel, S. Grieninger, A. Soloviev, J. Noronha, L. Noirez, W. van der Schee, I. Aniceto, and A. Zaccone for useful comments and suggestions. M. B. acknowledges the support of the Shanghai Municipal Science and Technology Major Project (Grant No. 2019SHZDZX01). L. L. acknowledges support from the National Natural Science Foundation of China Grants No. 12122513, No. 12075298, No. 11991052, and No. 12047503, and from the Key Research Program of the Chinese Academy of Sciences (CAS) Grant No. XDPB15 and the CAS Project for Young Scientists in Basic Research YSBR-006.

*b.matteo@sjtu.edu.cn
†liliphy@itp.ac.cn
‡sunhaotian@itp.ac.cn

[1] E. M. Purcell, Am. J. Phys. **45**, 3 (1977).
[2] K. Trachenko and V. Brazhkin, Phys. Today **74**, 66 (2021).
[3] P. K. Kovtun, D. T. Son, and A. O. Starinets, Phys. Rev. Lett. **94**, 111601 (2005).
[4] T. Schäfer and D. Teaney, Rep. Prog. Phys. **72**, 126001 (2009).
[5] J. L. Nagle, I. G. Bearden, and W. A. Zajc, New J. Phys. **13**, 075004 (2011).
[6] M. Luzum and P. Romatschke, Phys. Rev. C **78**, 034915 (2008).
[7] C. Shen, U. Heinz, P. Huovinen, and H. Song, Phys. Rev. C **84**, 044903 (2011).
[8] S. Cremonini, Mod. Phys. Lett. B **25**, 1867 (2011).
[9] S. A. Hartnoll, Nat. Phys. **11**, 54 (2015).
[10] K. Trachenko and V. V. Brazhkin, Sci. Adv. **6**, eaba3747 (2020).
[11] K. Trachenko, V. Brazhkin, and M. Baggioli, SciPost Phys. **10**, 118 (2021).
[12] K. Trachenko, M. Baggioli, K. Behnia, and V. V. Brazhkin, Phys. Rev. B **103**, 014311 (2021).
[13] R. P. Chhabra, *Rheology of Complex Fluids* (Springer, New York, 2010), pp. 3–34.
[14] R. S. Rivlin, Proc. R. Soc. A **193**, 260 (1948).
[15] K. J. Eskola, Nat. Phys. **15**, 1111 (2019).
[16] T. Schaefer, Annu. Rev. Nucl. Part. Sci. **64**, 125 (2014).
[17] J. Noronha-Hostler, J. Noronha, and M. Gyulassy, Phys. Rev. C **93**, 024909 (2016).
[18] A. Mazeliauskas and J. Berges, Phys. Rev. Lett. **122**, 122301 (2019).
[19] W. Busza, K. Rajagopal, and W. van der Schee, Annu. Rev. Nucl. Part. Sci. **68**, 339 (2018).

[20] W. Florkowski, M. P. Heller, and M. Spalinski, Rep. Prog. Phys. **81**, 046001 (2018).
[21] P. Romatschke, Phys. Rev. Lett. **120**, 012301 (2018).
[22] A. Behtash, C. N. Cruz-Camacho, S. Kamata, and M. Martinez, Phys. Lett. B **797**, 134914 (2019).
[23] A. Jaiswal and V. Roy, Adv. High Energy Phys. **2016**, 9623034 (2016).
[24] G. S. Denicol and J. Noronha, Nucl. Phys. **A1005**, 121748 (2021).
[25] G. S. Denicol and J. Noronha, Phys. Rev. D **99**, 116004 (2019).
[26] G. S. Denicol and J. Noronha, Phys. Rev. Lett. **124**, 152301 (2020).
[27] A. Kurkela, W. van der Schee, U. A. Wiedemann, and B. Wu, Phys. Rev. Lett. **124**, 102301 (2020).
[28] I. Aniceto, G. Basar, and R. Schiappa, Phys. Rep. **809**, 1 (2019).
[29] J. Casalderrey-Solana, H. Liu, D. Mateos, K. Rajagopal, and U. A. Wiedemann, *Gauge/String Duality, Hot QCD and Heavy Ion Collisions* (Cambridge University Press, Cambridge, England, 2014), 10.1017/CBO9781139136747.
[30] S. A. Hartnoll, A. Lucas, and S. Sachdev, arXiv: 1612.07324.
[31] M. Baggioli, *Applied Holography: A Practical Mini-Course*, SpringerBriefs in Physics (Springer, New York, 2019), 10.1007/978-3-030-35184-7.
[32] P. M. Chesler and L. G. Yaffe, Phys. Rev. Lett. **102**, 211601 (2009).
[33] M. P. Heller, R. A. Janik, and P. Witaszczyk, Phys. Rev. Lett. **108**, 201602 (2012).
[34] M. P. Heller, R. A. Janik, and P. Witaszczyk, Phys. Rev. D **85**, 126002 (2012).
[35] P. M. Chesler and L. G. Yaffe, J. High Energy Phys. 07 (2014) 086.
[36] J. Casalderrey-Solana, M. P. Heller, D. Mateos, and W. van der Schee, Phys. Rev. Lett. **111**, 181601 (2013).
[37] M. Attems, J. Casalderrey-Solana, D. Mateos, D. Santos-Oliván, C. F. Sopuerta, M. Triana, and M. Zilhão, J. High Energy Phys. 01 (2017) 026.
[38] J. K. Ghosh, S. Grieninger, K. Landsteiner, and S. Morales-Tejera, Phys. Rev. D **104**, 046009 (2021).
[39] S. Morales-Tejera and K. Landsteiner, Phys. Rev. D **102**, 106020 (2020).
[40] J. Fernández-Pendás and K. Landsteiner, Phys. Rev. D **100**, 126024 (2019).
[41] K. Landsteiner, E. Lopez, and G. Milans del Bosch, Phys. Rev. Lett. **120**, 071602 (2018).
[42] S. L. Grieninger, Non-equilibrium dynamics in holography, Ph.D. thesis, Jena University, 2020, 10.22032/dbt.45425.
[43] M. Ammon, S. Grieninger, A. Jimenez-Alba, R. P. Macedo, and L. Melgar, J. High Energy Phys. 09 (2016) 131.
[44] M. P. Heller and M. Spalinski, Phys. Rev. Lett. **115**, 072501 (2015).
[45] A. Kurkela, W. van der Schee, U. A. Wiedemann, and B. Wu, Phys. Rev. Lett. **124**, 102301 (2020).
[46] Z. Du, X.-G. Huang, and H. Taya, Phys. Rev. D **104**, 056022 (2021).
[47] M. Strickland, J. Noronha, and G. S. Denicol, Phys. Rev. D **97**, 036020 (2018).
[48] M. Spaliński, Phys. Lett. B **776**, 468 (2018).
[49] P. Kovtun, J. Phys. A **45**, 473001 (2012).
[50] B. Bradlyn, M. Goldstein, and N. Read, Phys. Rev. B **86**, 245309 (2012).
[51] D. T. Son and A. O. Starinets, Annu. Rev. Nucl. Part. Sci. **57**, 95 (2007).
[52] G. Policastro, D. T. Son, and A. O. Starinets, J. High Energy Phys. 09 (2002) 043.
[53] D. T. Son and A. O. Starinets, J. High Energy Phys. 09 (2002) 042.
[54] D. Zubarev, D. Zubarev, P. Gray, P. Shepherd, and P. Gray, *Nonequilibrium Statistical Thermodynamics*, Studies in Soviet Science: Physical Sciences (Springer, New York, 1974).
[55] A. Puglisi, A. Sarracino, and A. Vulpiani, Phys. Rep. **709**, 1 (2017).
[56] Y. Demirel, *Nonequilibrium Thermodynamics: Transport and Rate Processes in Physical, Chemical and Biological Systems* (Elsevier, New York, 2007).
[57] J. D. Bekenstein, Phys. Today **33**, 24 (1980).
[58] R. Rougemont, W. Barreto, and J. Noronha, Phys. Rev. D **105**, 046009 (2022).
[59] I. Booth, Can. J. Phys. **83**, 1073 (2005).
[60] D. Forster, D. R. Nelson, and M. J. Stephen, Phys. Rev. A **16**, 732 (1977).
[61] S. A. Hartnoll, Classical Quantum Gravity **26**, 224002 (2009).
[62] L. Alberte, M. Baggioli, A. Khmelnitsky, and O. Pujolas, J. High Energy Phys. 02 (2016) 114.
[63] L. Alberte, M. Baggioli, and O. Pujolas, J. High Energy Phys. 07 (2016) 074.
[64] M. Baggioli, Gravity, holography and applications to condensed matter, Ph.D. thesis, Universitat Autònoma de Barcelona, 2016, arXiv:1610.02681.
[65] T. Andrade, M. Baggioli, and O. Pujolàs, Phys. Rev. D **100**, 106014 (2019).
[66] M. Baggioli and S. Grieninger, J. High Energy Phys. 10 (2019) 235.
[67] M. Baggioli, K.-Y. Kim, L. Li, and W.-J. Li, Sci. China Phys. Mech. Astron. **64**, 270001 (2021).
[68] L. Li, Phys. Lett. B **815**, 136123 (2021).
[69] See Supplemental Material at http://link.aps.org/supplemental/10.1103/PhysRevLett.129.011602 for more details about the holographic models, the technical computations and the numerical methods.
[70] A. C. Pipkin, *Lectures on Viscoelasticity Theory* (Springer-Verlag, New York, 1972), pp. viii, 180 p.
[71] M. Baggioli, S. Grieninger, and H. Soltanpanahi, Phys. Rev. Lett. **124**, 081601 (2020).
[72] M. F. Wondrak, M. Kaminski, and M. Bleicher, Phys. Lett. B **811**, 135973 (2020).
[73] P. Arnold, P. Romatschke, and W. van der Schee, J. High Energy Phys. 10 (2014) 110.
[74] P. Romatschke, J. High Energy Phys. 12 (2017) 079.
[75] C. Chattopadhyay, S. Jaiswal, L. Du, U. Heinz, and S. Pal, Phys. Lett. B **824**, 136820 (2022).
[76] Z. Chen and L. Yan, Phys. Rev. C **105**, 024910 (2022).
[77] H. Liu, The Reasonable and Unreasonable Effectiveness of Hydrodynamics in Exotic Quantum Matter, 2020, http://shovkovy.faculty.asu.edu/colloquium/slides/Colloquium_Slides_Liu.pdf.

[78] J. Noronha-Hostler, J. Noronha, and M. Gyulassy, Nucl. Phys. **A956**, 890 (2016).
[79] M. P. Heller, Acta Phys. Pol. B **47**, 2581 (2016).
[80] P. Romatschke, Int. J. Mod. Phys. E **19**, 1 (2010).
[81] D. Pan, T. Ji, M. Baggioli, L. Li, and Y. Jin, Sci. Adv. **8**, eabm8028 (2022).
[82] O. DeWolfe, S. S. Gubser, C. Rosen, and D. Teaney, Prog. Part. Nucl. Phys. **75**, 86 (2014).